J Sol-Gel Sci Technol (2013) 68:213–218
DOI 10.1007/s10971-013-3154-y

Preparation and photocatalytic antibacterial property of nitrogen doped TiO_2 nanoparticles

Pingting He · Jie Tao · Xianli Huang · Jianjun Xue

Received: 12 May 2013 / Accepted: 6 September 2013 / Published online: 18 September 2013

Abstract Nitrogen doped TiO_2 (N-TiO_2) nanoparticles with about 30 nm in size were produced by a sol–gel method and characterized respectively by UV–vis, X-ray diffraction (XRD), Transmission electron microscopy, X-ray photoelectron spectroscopy (XPS). Their photocatalytic antibacterial properties were evaluated by the antibacterial ratio against *Escherichia coli* in dark and under simulated sunlight respectively. The XRD pattern showed that the doped nano-TiO_2 was mainly composed of anatase phase. The XPS spectra of the N-TiO_2 sample indicated that TiO_2 was doped by nitrogen atom. The nitrogen doping created a new N 2p state slightly above the valence band top consists of O 2p state, and this pushes up the valence band top and decreased the band gap. Which leaded to the absorption edge was red-shifted to the visible light region of UV–vis spectra of nitrogen doped nano-TiO_2 comparing with pure nano-TiO_2. The antibacterial percentage of N-TiO_2 against *E. coli* reached to 90 % under simulated sunlight for 2 h, which was much better than that in dark, also than that of pure nano-TiO_2. The photo-catalytic antibacterial activity was activated under visible light. The structure and integrity of cell wall and cell membrane were destructed, and even caused the bacteria death.

Keywords Inorganic antibacterial agent · Titanium dioxide · Doped with inorganic non-metal elements · Photocatalysis

1 Introduction

A new avenue for water sterilization has been created, since Matsunaga and co-workers [1] reported that microbial cells in water could be killed by contact with a TiO_2-Pt photocatalyst upon irradiation with UV light for 60–120 min in 1985. TiO_2-mediated disinfection seems to be a promising technique compared to the common disinfection methods such as chlorination and UV disinfection. For the shortcoming of the methods and the emergence of more resilient and virulent strains of microorganisms, it is need for more effective sterilization technologies and antibacterial materials.

The primary event occurring on the illuminated TiO_2 is the generation of e^-_{cb}(photogenerated electrons) and h^+_{vb}(photogenerated holes). In these reactions, the organic matter are oxidized by the photogenerated holes or by reactive oxygen species such as ·OH and O_2^- radicals formed on the irradiated TiO_2 surface [2]. However, it is a problem in the application of TiO_2 as a photocatalyst that the band gap energy of TiO_2 is too large, i.e. the band gap value of anatase is 3.2 eV so that it only shows photocatalytic activity under near-UV region($\lambda \leq 390$ nm), which is about 3 % of the solar spectrum. Due to this inherent

P. He (✉) · J. Tao · X. Huang · J. Xue
College of Materials Science and Technology, Nanjing University of Aeronautics and Astronautics, Nanjing 210016, China
e-mail: hepingting@nuaa.edu.cn

J. Tao
e-mail: taojie@nuaa.edu.cn

X. Huang
e-mail: xianlihuang@163.com

J. Xue
e-mail: jjxue@nuaa.edu.cn

X. Huang
State Environmental Protection Key Laboratory of Microorganism Application and Risk Control (MARC), Tsinghua University, Beijing 100084, China

limitation, solar energy cannot be utilized efficiently for photocatalytic disinfection.

To improve the efficiency, a new approach to broaden the photoresponse of TiO_2 by doping with a nonmetal atom has been introduced. Recently, some groups have reported that nonmetal doped into TiO_2 such as boron [3], carbon [4], nitrogen [5], fluorine [6], sulfur [7, 8], chlorine and bromine [9], iodine [10] to achieve enhanced visible light photocatalytic activities undeniably, doping TiO_2 photocatalyst with a nonmetal element becomes a hot research topic, and it opens up new possibilities for the development of solar-induced photocatalytic materials.

Asahi et al. [11] reported theoretical calculations of the band structure of nitrogen-doped TiO_2 and its visible light photocatalytic degradation of acetaldehyde and methylene blue. Henceforth, several groups [12–16] investigated the photocatalytic and photo-electrochemical properties of nitrogen-doped TiO_2 powders and thin films prepared by different methods.

Although the use of TiO_2 in disinfection and the photocatalytic degradation organic pollutants has been studied extensively, there has been no report regarding the visible-light-induced bactericidal effects of TiO_2 doped with a nonmetal element. The information about this visible-light induced disinfection is both scientifically and practically important. We believe that the nonmetal doping is a promising approach to improve the efficiency of TiO_2 disinfection. In the present work, we reveal that nitrogen-doped TiO_2 powder exhibits bactericidal effects on *Escherichia coli* under visible light irradiation.

2 Materials and methods

2.1 Preparation and characterization of N-TiO_2

Nitrogen-doped TiO_2 was prepared by sol–gel methods. Tetrabutyl titanate ($(Ti(O(CH_2)_3–CH_3)_4$, TBT) as Ti source and urea as nitrogen source were dissolved in absolute ethanol under vigorous stirring, respectively. And the pH value of solution was adjusted to 2–3 by addition of glacial acetic acid. After being stirred for 30 min, some water was dropping into the mixed solution with 1 mL/min, and the gel was obtained by hydrolysis. The gel was dried and thermal-treated to crystallize. The solid was ground to a powder with an agate mortar.

The X-ray diffraction (XRD, Bruker, D8 advance) patterns were used to identify the phase constitutions in samples and their crystallite size. UV–vis diffuse reflectance spectra were achieved by a UV–vis spectrophotometer (Shimadzu, UV3600). Morphologies of samples were characterized using a transmission electron microscopy (FEI, Tecnai 20). The XPS measurement was performed by an X-ray photoelectron spectrometer (VG, EscalabMK II).

2.2 Antimicrobial property evaluation of nanoparticles

We consulted ISO 22196-2007 and the National Standard GB/T 21510-2008 of the people's republic of China to evaluate the antimicrobial property of TiO_2 nanoparticles. *E. coli* ATCC 8099 was used as a model microorganism for all inactivation studies. It was assumed that one cell (or one cluster of cells) will multiply on the medium to produce a visible colony. One milliliter diluted suspension with a final cell concentration of 10^5 cfu/mL was mixed with the required amount of nano-TiO_2 suspension, after a period then plating 0.5 mL of each mixed solution onto nutrient agar in triplicate, and counting the resultant colonies. The survival ratio of germ was calculated as follow formula:

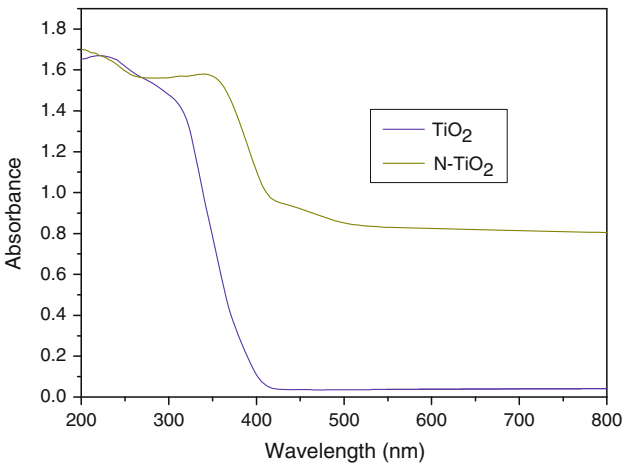

Fig. 1 UV-vis diffuse reflectance spectra of TiO_2 and N-TiO_2

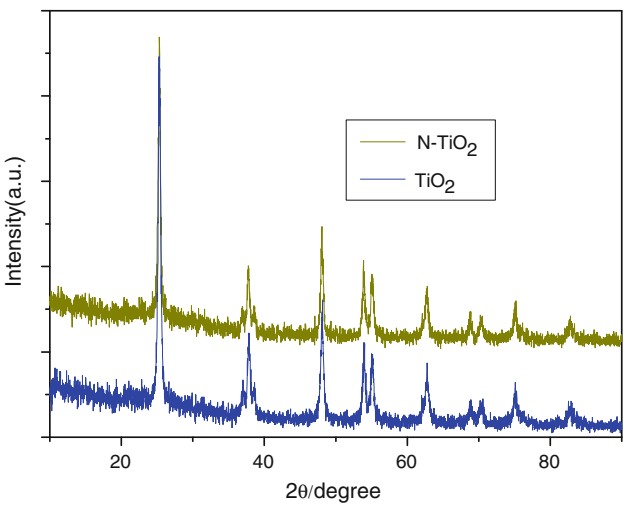

Fig. 2 X-ray diffraction pattern of nano TiO_2 and N-TiO_2

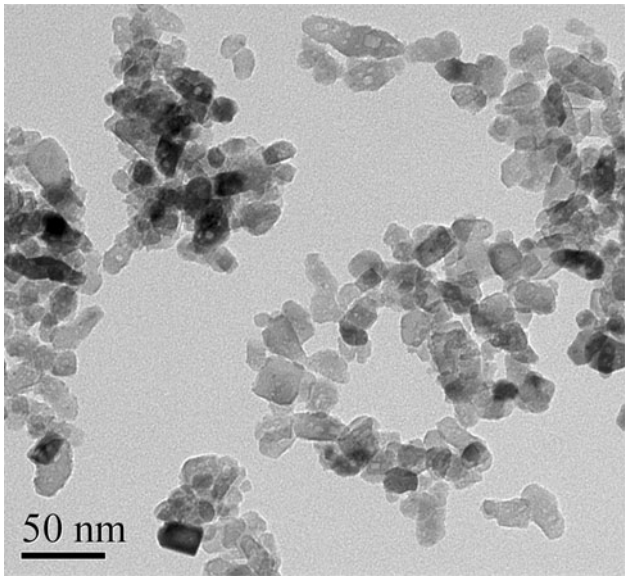

Fig. 3 TEM images of Nitrogen-doped TiO_2 samples

$$R(\%) = \frac{N}{N_0} \times 100\,\%$$

R represents the survival rate of bacterium; N and N_0 mean the colony number of each sample group and positive group, respectively.

The antibacterial property evaluation against *E. coli* was carried out under simulated sunlight and dark. The xenon lamp (300 W, 15 mA) was used as simulated sunlight with a cutoff filter ($\lambda > 420$ nm) to block the passage of UV light, and in dark the incubator was enveloped with aluminium foil.

Scanning electron microscopy (SEM, FEI, Quanta200) imaging was carried out as follows [17]: *E. coli* cultures in the late exponential growth phase (OD 0.7–0.9) exposed to nanoparticles were collected and fixed with 2.5 % glutaradehyde in phosphate buffer at pH 7.2 for 4 h. Fixed samples were rinsed in buffer. Dehydration of sample was carried out through increasing ethanol concentrations of alcohol and water solution from 30, 50, 70, 85, 95 % to

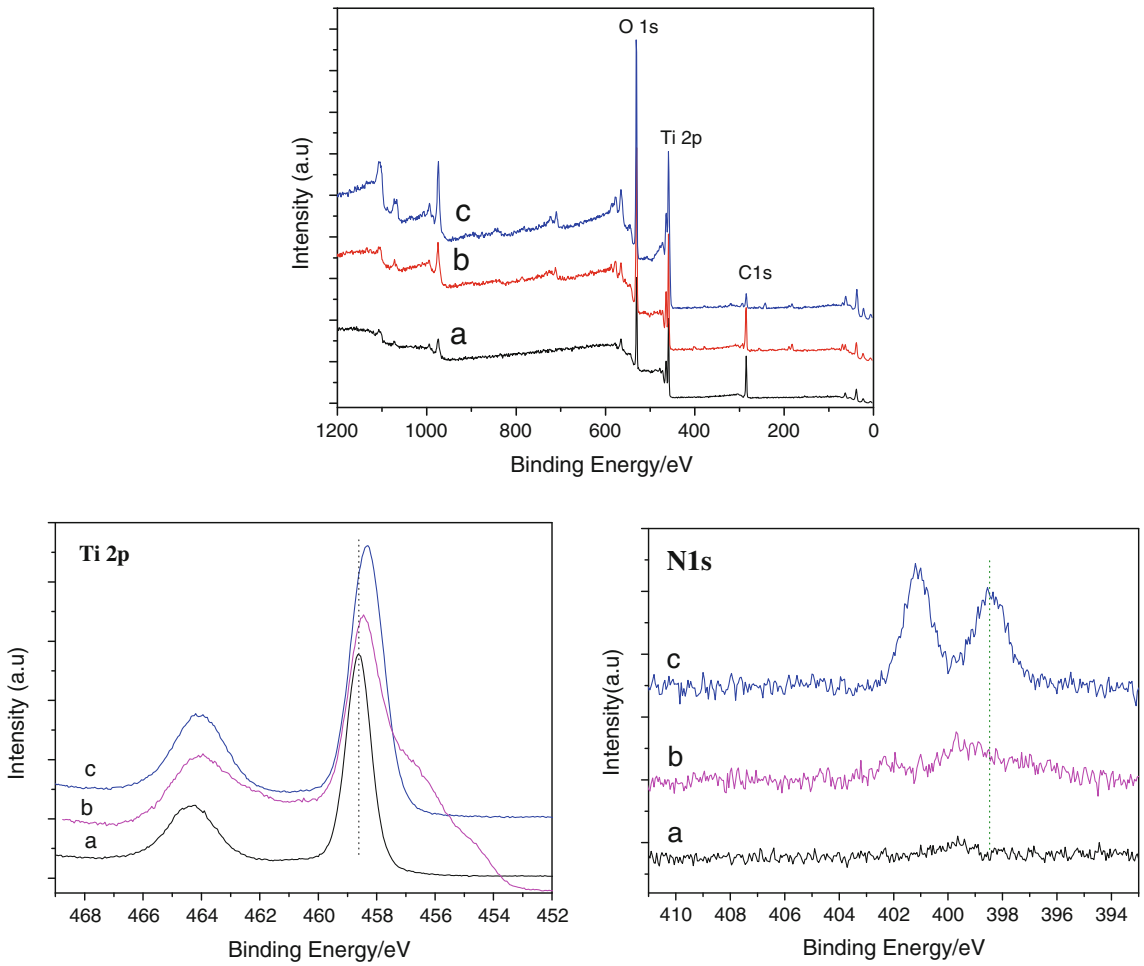

Fig. 4 XPS Survey spectra and high resolution XPS spectra for Ti 2p and N 1 s spectra of undoped TiO_2 and N-doped TiO_2. (**a**) the undoped TiO_2, (**b**) the N-doped TiO_2 specimen etched for 300 s, (**c**) the N-doped TiO_2

absolute alcohol, then the obtained sample was fixed on microscope slide and coated with 1.2 nm of aurum in a sputter coater. Images were collected with an Apollo 300 field emission scanning electron microscope, operated at 10 kV.

3 Results and discussions

3.1 Characterization of N-TiO_2

Figure 1 shows the UV–vis diffuse reflectance spectra of the undoped TiO_2 and N-doped TiO_2 samples. The undoped TiO_2 is white in color and shows absorption only in the UV region ($\lambda < 390$ nm). The energy band gap estimated from the sharp absorption edge is 3.2 eV. The nitrogen-doped TiO_2 samples are yellowy and their optical absorption was extended to the visible region. It is noted that the band gap was expanded from 380 to 480 nm upon N doping. Noticeable shifts of the absorbance shoulder from a wavelength below 400 nm to the visible light region were observed for the N-doped TiO_2. The main absorption edges of the N-doped TiO_2 change significantly compared to that of the undoped sample. It is likely that nitrogen doping creates a new N 2p state slightly above the valence band top consists of O 2p state, and this pushes up the valence band top and leads to visible light response as a consequence [18, 19]. Undoubtedly, these results reveal that the nitrogen element are indeed incorporated into the lattice of TiO_2, thus altering its crystal and electronic structures.

XRD patterns of the as-prepared nanophase undoped TiO_2 and N-doped TiO_2 powders are shown in Fig. 2. All diffraction peaks of undoped TiO_2 and N-doped TiO_2 can be assigned to anatase TiO_2 and the diffraction data are in good agreement with the JCPDS card for titania (JCPDS No. No. 73-1764). The five major peaks locate at about 25.2°, 37.8°, 47.9°, 54.0°, and 62.7°. The crystal form of undoped TiO_2 and N-doped TiO_2 is anatase. Theoretically as the effective ionic radius of nitrogen (146 pm, consult the Lange's Chemistry Handbook version 15th) is slightly over that of oxygen (138 pm, consult the Lange's Chemistry Handbook version 15th), the doping could lead to the interplanar spacing becoming greater. However from the Fig. 2, comparing the diffraction angle of undoped TiO_2 and N-doped TiO_2, the differences are not distinguished.

As the penetrability of ultraviolet ray is less than X-ray, the UV–vis diffuse reflectance spectra reflect the optical absorption of particles surface layer, but the X-ray can penetrate through a certain range of thickness so that the XRD patterns can show the state of things inside the particles. Integrated the results of UV–vis scan and the XRD,

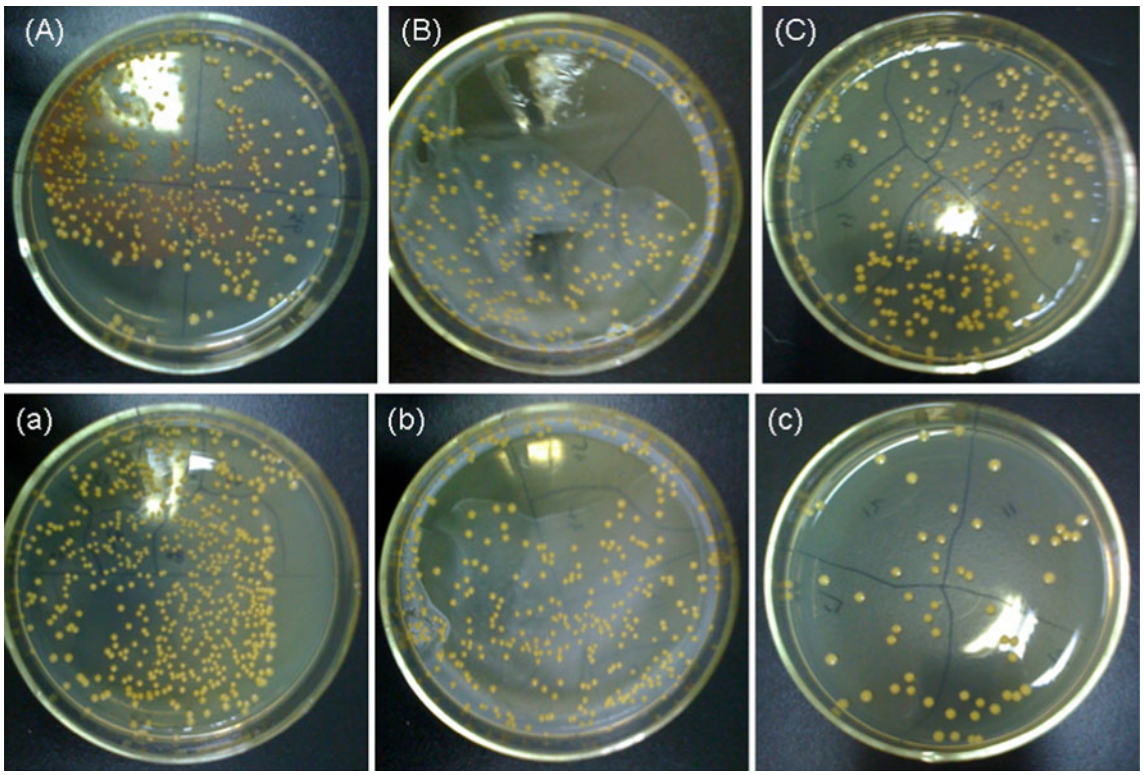

Fig. 5 Images of *Escherichia coli* colonies on an agar plate (**A**–**C**) are in the dark for 24 h, and (**a**–**c**) are under visible light irradiation for 2 h. (**A** and **a**) controls, (**B** and **b**) undoped TiO_2, (**C** and **c**) N-doped TiO_2

the nitrogen doping is happened mostly on the surface layer of TiO_2 particles, and majority of undoped TiO_2 is in the particle core.

Transmission electron microscopy (TEM) was used to investigate the exact microstructure of samples. From Fig. 3, we can see that the nitrogen-doped TiO_2 sample consists of uniform nanoparticles with average diameter of 20–30 nm.

To explore the states of the doped nitrogen species, the nitrogen-doped samples were subjected to X-ray photoelectron spectroscopy (XPS) analysis. Figure 4 shows the XPS survey spectrum of the undoped TiO_2 and N-TiO_2 sample. Obviously, Ti, O, and C elements exist at the surface of the sample, whereas the peak intensity is different. Figure 4 depicts the N 1 s XPS spectra of N-TiO_2 with 20 scans, showing the peaks at the binding energy positions of 380–404 eV. After doping with N, two peaks are observed at binding energy of 398.5 and 401.2 eV. From previous reports [20–22], the binding energy peaks at 398.5 eV is attributed to anionic N doping incorporated into TiO_2 as an O–Ti–N structural feature. The O–Ti–N linkage is a typical substitutional N doping, which has been reported to be due to N atoms within NH_3 being bonded to Ti atoms and replacing lattice oxygen atoms in the TiO_2. The higher binding energy peaks at 401.2 eV can be assigned to Ti–O–N. After the N-TiO_2 specimen was etched by Ar ion for 300 s, a layer of about 10 nm thicknesses was removed from the particle surface, and the N 1 s peak for N doping exist still but it is less obvious and the intensity is weaken, so we think the nitrogen doping is happened mostly on the surface layer of particles, and majority of undoped TiO_2 is in the particle core. From the high resolution XPS spectra for Ti 2p, it can be seen that Ti 2p spectra consists of two peaks at around 458.7 eV (Ti 2p3/2) and 464.2 eV (Ti 2p1/2). Ti 2p region showed that Ti was in +4 states, which was confirmed by the oxidation of Ti to TiO_2. The peak at 458.7 eV becomes broader and unsymmetrical after N doping, in addition the binding energy is increased [23]. These indicate that a Ti +3 state is present due to the vacancies created by the nitrogen doping. However the change becomes indistinct after the N-TiO_2 specimen was etched. So the N doping is happened on the surface layer of TiO_2 particles, and producing numerous defects and lattice vacancies. But in the particle core, the undoped TiO_2 is available in abundance. The nitrogen concentration can not be detected by only one scan at the surface of the sample for it is not homogeneous.

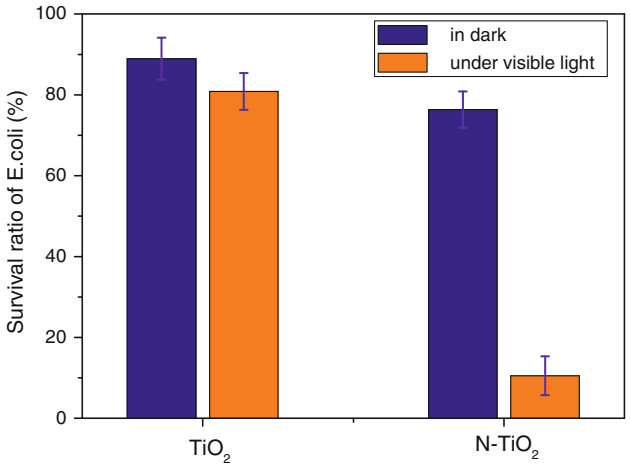

Fig. 6 The survival ratio of *E. coli* exposed to undoped TiO_2 and N-TiO_2

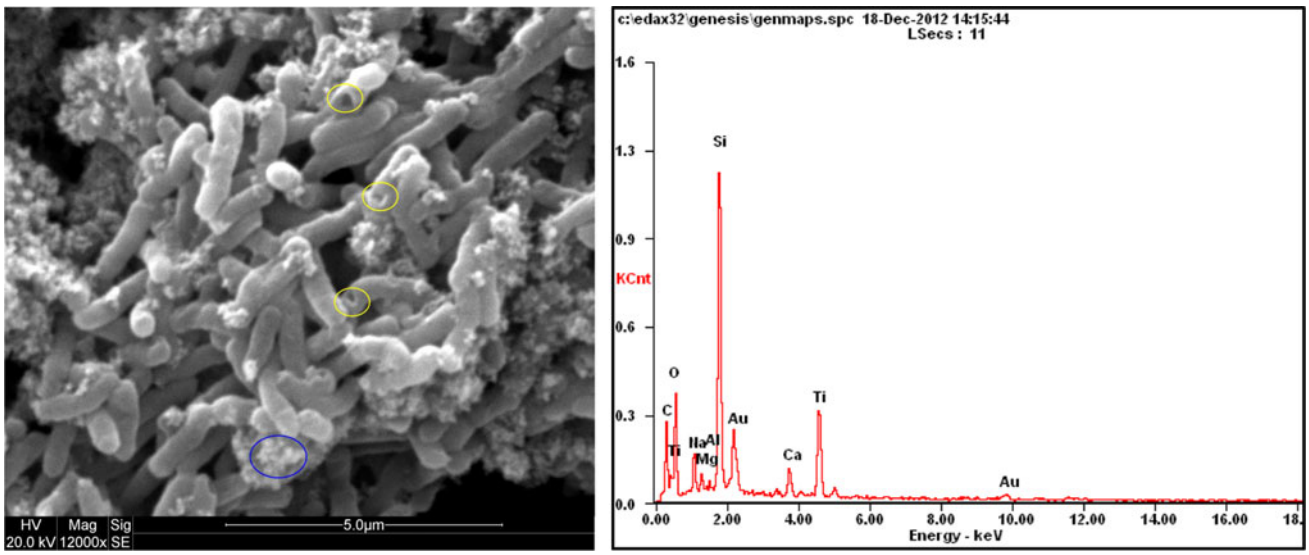

Fig. 7 SEM Images of *E. coli* exposed to N-TiO_2 and EDS of aggregate

3.2 Antimicrobial property of N-TiO_2 nanoparticles

The antibacterial activities of the samples were evaluated by the killing of *E. coli* in water under visible light irradiation on the basis of the decrease in the colony number of *Escherichia coli* formed on an agar plate.

According to the Figs. 5 and 6, the survival ratio of *E. coli* can be decreased to 8.75 % within 2 h N-doped TiO_2 nanoparticles under visible light irradiation. Neither undoped TiO_2 nor N-doped TiO_2 in the dark for 24 h shows any bactericidal effects on *E. coli*, indicating that the photocatalyst itself is not toxic to *E. coli*. Thus, the bactericidal effect is ascribed to the photocatalytic reaction of the N-doped TiO_2.

The photocatalytic antibacterial activity of the N-doped is obvious under visible irradiation. Visible light activity in N-doped TiO_2 may be caused by band-gap narrowing from mixing the N 2p states with O 2p states. The phenomenon of band-gap narrowing in nonmetal atom doped TiO_2 has been reported in the literatures [24, 25].

In addition, possible mechanisms for the bactericidal effect of TiO_2 photocatalysis have been proposed. The photocatalysts are activated at the sub-band gap energy when exposed to visible light and generate reactive oxygen species such as hydroxyl radicals. These hydroxyl radicals cause various damages to living organisms [26]. Further study about the generation of hydroxyl radical levels from N-doped TiO_2 under visible light irradiation is currently in progress.

From Fig. 7, we can see that the nanoparticles aggregated upon the cells, and the EDS characterization of the aggregate indicates that it was TiO_2 (blue circle), some cells showed substantial damage (yellow circle points to the damaged part of the cell). It has been reported previously that the fullerene compounds might have caused the destruction of membrane integrity in bacteria [17]. Moreover, the aggregation of organism was associated with oxidative stress and aggregation could be a protection mechanism. On the other hand, bacteria may produce certain membrane proteins to strengthen its membrane structure in response to nanoparticle stress to reduce its membrane's permeability. This observation was consistent with previous evidence that fullerene compounds intercalate into the cell wall and cell membrane in some Gram-negative bacteria.

4 Conclusions

In conclusion, the goals both of extending the TiO_2 spectral response to the visible region and of improving its photocatalytic activity were realized by doped with nitrogen. The photocatalyst antibactericidal activity showed much higher photoreactivity than undoped TiO_2 both on *E. coli* under visible light irradiation. This study demonstrated a novel approach for the efficient utilization of visible light in killing bacteria through doping nitrogen into TiO_2 photocatalyst. The photo-catalytic antibacterial activity was activated under visible light, and the generated hydroxyl radicals from the N-doped TiO_2 leaded to considerable bactericidal effects on *E. coli*. The structure and integrity of cell wall and cell membrane were destructed so that the bacteria were killed.

Acknowledgments This work was financially supported by the Fundamental Research Funds for the Central Universities (NO. NS2012113) and State Environmental Protection Key Laboratory of Microorganism Application and Risk Control open fund (No. MARC2011D043).

References

1. Matsunaga T, Tomoda R, Nakajima T, Wake H (1985) FEMS Microbiol Lett 29:211–214
2. Linsebigler AL, Lu G, Yates JT (1995) Chem Rev 95:735–758
3. In S, Orlov A, Berg R, García F, Jimenez SP, Tikhov MS, Wright DS, Lambert RM (2007) J Am Chem Soc 129:13790–13791
4. Irie H, Watanabe Y, Hashimoto K (2003) Chem Lett 32:772–773
5. Asahi R, Morikawa T, Ohwaki T, Aoki K, Taga Y (2001) Science 293:269–271
6. Czoska AM, Livraghi S, Paganini MC, Giamello E, Di Valentin C, Granozzi G (2011) Phys Chem Chem Phys 13:136–143
7. Umebayashi T, Yamaki T, Itoh H, Asai K (2002) Appl Phys Lett 81:454–456
8. Lin XX, Fu DG (2012) Adv Mater Res 374:895–898
9. Luo H, Takata T, Lee Y, Zhao J, Domen K, Yan Y (2004) Chem Mater 16:846–849
10. Wang Z, Cai W, Hong X, Zhao X, Xu F, Cai C (2005) Appl Catal B 57:223–231
11. Asahi R, Morikawa T (2007) Chem Phys 339:57–63
12. Shi H, Li X, Iwai H, Zhou Z, Ye J (2009) J Phys Chem Solids 70:931–935
13. Shao G, Wang F, Ren T (2009) Appl Catal B 92:61–67
14. Akpan UG, Hameed BH (2010) Appl Catal A 375:1–11
15. Shi H, Zhang T, Wanng H (2011) J Rare Earths 29:746–752
16. Tsao N, Luh TY, Chou CK (2002) J Antimicrob Chemother 49:641–649
17. Tang YJ, Ashcroft JM, Ding Chen (2007) Nano Lett 7:754–760
18. Nosaka Y, Matsushita M, Nishino J, Nosaka AY (2005) Sci Technol Adv Mater 6:143–148
19. Livraghi S, Paganini MC, Giamello E, Selloni A, Valentin CD, Pacchioni G (2006) J Am Chem Soc 128:15666–15671
20. Ou HH, Lo SL, Liao CH (2011) J Phys Chem C 115:4000–4007
21. Valentin CD, Finazzi E, Pacchioni G, Selloni A, Livraghi S, Paganini MC, Giamello E (2007) Chem Phys 339:44–56
22. Qiu X, Zhao Y, Burda C (2007) Adv Mater 19:3995–3999
23. Junna Xu, Liu Qing, Lin Shufeng, Cao Wenbin (2013) Res Chem Intermed 39:1655–1664
24. Lin L, Zheng RY, Xie JL, Zhu YX, Xie YC (2007) Appl Catal B 76:196–202
25. Akpan UG, Hameed BH (2010) Appl Catal A 375:1–11
26. Li X, Zhuang Z, Li W, Pan H (2012) Appl Catal A 429–430:31–38